Journal of the Korean Physical Society, Vol. 74, No. 12, June 2019, pp. 1184∼1189

Photovoltaic Modules Using a Galinstan Paste Interconnection

Hyeon Soo Cho
Photovoltaic Laboratory, Korea Institute of Energy Research, Daejeon 34129, Korea and School of Chemical Engineering, Sungkyunkwan University (SKKU), Suwon 16419, Korea

Jeong In Lee, Sungeun Park and Hee-eun Song
Photovoltaic Laboratory, Korea Institute of Energy Research, Daejeon 34129, Korea

Dong-Youn Shin
Department of Graphic Arts Information Engineering, Pukyong National University, Busan 48513, Korea

Tae-il Kim
School of Chemical Engineering, Sungkyunkwan University (SKKU), Suwon 16419, Korea

Min Gu Kang*
Photovoltaic Laboratory, Korea Institute of Energy Research, Daejeon 34129, Korea

(Received 17 December 2018, in final form 8 February 2019)

A shingled silicon photovoltaic (PV) module without busbars on the front side of a solar cell can increase the light-receiving area and provide more power than a conventional PV module. However, there are several issues, such as damage by laser cutting and interconnection by conductive paste. As the number of busbars increases, the laser cutting process increases, and this process damages the solar cell. Additionally, the interconnection process increases as the number of busbars increases. On the other hand, as the number of busbars increases, the finger length can decrease, and the resistance decreases. In this research, a shingled silicon PV module was fabricated by interconnecting of 6 unit cells with various finger and busbar patterns. Photoluminescence, electroluminescence, light current-voltage characteristics and quantum efficiency were used to observe the damage caused by the laser cutting process. Furthermore, we optimized the electrode pattern design for the shingled silicon PV module. The connecting material is very important for electrically connecting the cut unit cell. We used electrical conductive adhesive (ECA) and Galinstan as the interconnection materials. ECA is the most commonly used material for interconnections; in contrast, Galinstan, a liquid metal, is not commonly used as an interconnection material. Therefore, we compared ECA with Galinstan in the shingled silicon PV module. A liquid silicone module method was used to fabricate the module because that method uses a lower pressure and temperature than a conventional silicon PV module process.

PACS numbers: 88.40.H−, 88.40.hj, 88.40.jj
Keywords: Shingled module, Crystalline silicon solar cell, Galinstan
DOI: 10.3938/jkps.74.1184

I. INTRODUCTION

A solar cell is a semiconductor device that converts light energy into electric energy and should be manufactured in the form of a module to function for a long time without being affected by exposure to external environments. In a typical solar cell module, solar cells are connected in series with each other by using a ribbon. Materials such as ethyl vinyl acetate (EVA), back sheet, and glass are laminated by applying heat on both ends of the solar cells for protection, and finally, the module is completed within a frame [1].

At this point, the loss that occurs during the manufacturing process of the solar cell module depends on the resistance of the ribbon that connects the solar cell, the contact resistance between the ribbon and the solar cell electrode, the shadow loss due to the electrode and the ribbon, and the area loss occurring at the in-

*E-mail: mgkang@kier.re.kr

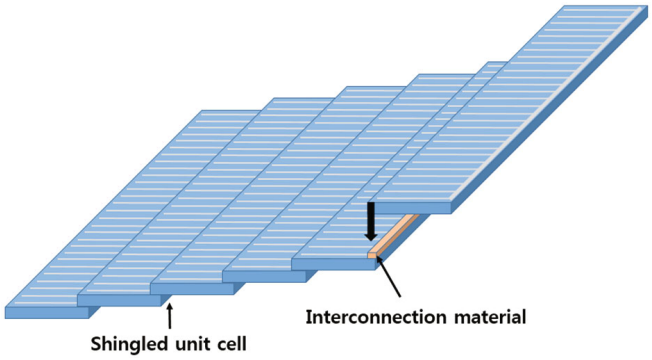

Fig. 1. (Color online) Schematic diagram of an interconnected string of shingled modules.

tervals between the solar cells [2–4]. One of the ways to reduce these losses is to fabricate a module by using a laser to cut high-efficiency solar cells within each unit cell and then connect the unit cells directly within a shingled structure without using a ribbon [5,6]. The shingled module has the advantage of producing more electric power per area than currently commercialized modules because the former eliminates the contact resistance due to the ribbon, the shadow loss caused by the busbar and the gap between each solar cell.

A pattern different from that of a conventional solar cell is used to fabricate a shingled module. Because the busbar of a conventional solar cell exists at the same position on both sides of the solar cell, the ribbon is connected in a serial connection, but the busbar of the unit cell used for the shingled module is located at the edges of both sides of the cell. Therefore, each cell is connected using electrically conductive adhesives (ECAs). In this case, the ECA, which is a conductive epoxy material, has high electrical conductivity, a high content of silver and a high unit price and should be stored at −20°C to prevent epoxy hardening [7]. Additionally, because the shingled module is heated and cured during the fabrication process, cell breakage or damage may occur [8,9]. Therefore, when fabricating a solar cell module by using the liquid metal Galinstan as a connecting material for a thin crystal silicon solar cell, damage due to the difference in the thermal expansion coefficients between the cell and the ribbon can be prevented [10]. Because Galinstan is much cheaper than Ag particles, Galinstan as an interconnection material has an advantages in fabrication cost. Moreover, by using liquid silicone, breakage that may be caused by the difference between the manufacturing of the shingled module and the unit cell may be prevented. In this study, we fabricated a shingled module by using Galinstan paste and liquid silicone and confirmed any damage that might have occurred during the manufacturing of the module, as well as the differences in the module's characteristics.

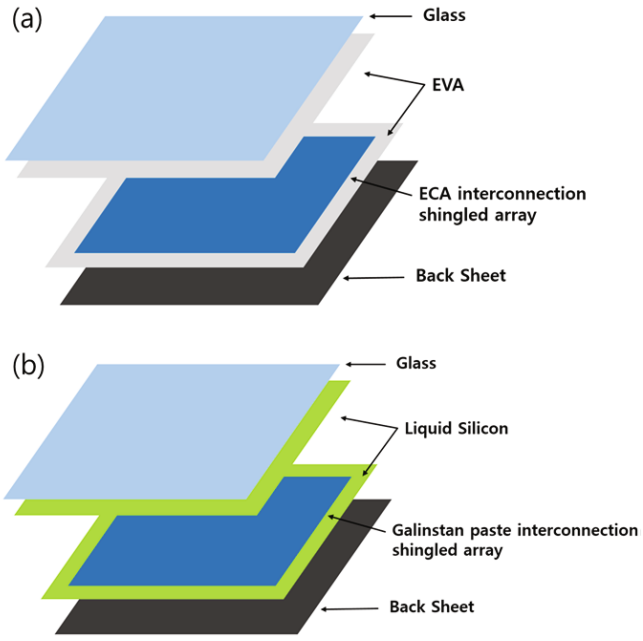

Fig. 2. (Color online) Schematic diagrams of (a) the EVA lamination module and (b) the liquid silicone module.

II. EXPERIMENTS AND DISCUSSION

In this experiment, solar cells with a passivated emitter and rear cell (PERC) structure were used to fabricate the shingled module. The PERC solar cell was fabricated with a 6-inch wafer, and the position of the busbar was printed on both edges of the solar cell after having cut off the solar cell to fabricate the shingled module [11]. As shown in Fig. 1, each unit cell was split into sizes of 26.00 mm × 156.75 mm by using a laser [12], and shingled modules were manufactured directly with 6 unit cells connected using either Galinstan or ECA from the Henkel Company [13,14].

As shown in Fig. 2, in the solar cell module fabricated using ECA, after the ECA had been applied to the busbar of the light-receiving part of the unit cell by using an air pressure dispenser and after having placed the busbar on the back of the other unit cell, heat treatment was performed at 180°C for 10 minutes, and the bonding was repeated to complete the string. The solar cell was wired at both ends of the string by tabbing the ribbon and was laminated in the order of glass, EVA, solar cell string, EVA, and back sheet; then, the solar cell was laminated at 110°C for 20 minutes to complete the module.

However, because Galinstan itself has a very high surface tension and is difficult to print, it was fabricated as a paste and used [15]. Galinstan paste was prepared by mixing Galinstan 95%, PD-2246 0.95%, ethyl cellulose 0.28%, Thixatrol Max 0.48%, terpineol 2.3%, and butyl carbitol acetate 0.99% [7]. The produced paste was applied to the pneumatic dispenser on the busbar of the unit cell; then, this paste abutted the busbar on the back

Table 1. Photocurrent-voltage characteristics of shingled modules using ECA and Galinstan as interconnection materials before and after thermal cycle testing.

	V_{oc} (V)	I_{sc} (A)	P_{max} (W)	FF (%)	Efficiency (%)	Rs (Ω)	Rsh (Ω)
ECA TC 0 cycle	3.92	1.48	4.26	74.1	18.2	0.298	143
Galinstan TC 0 cycle	3.93	1.44	4.25	74.9	18.6	0.278	2295
ECA TC 200 cycles	3.90	1.46	3.54	63.2	15.7	0.387	167
Galinstan TC 200 cycles	3.91	1.42	3.83	69.8	16.8	0.270	276

of the other unit cell. After the cell and Galinstan paste had been positioned, curing was performed for 3 minutes with a hot plate heated to 150°C to remove any organic matter from the paste. Unlike the ECA, the Galinstan paste was laminated with liquid silicone instead of EVA because EVA could not adhere to the solar cell. Liquid silicone was used after mixing a liquid silicone base and curing agent, stirring for 2 minutes and defoaming at 2,000 rpm 30 seconds. Liquid silicone was applied to half of the back sheet and half of the front glass. The shingled sample was put together and bonded; then, the liquid silicone was cured for approximately 10 minutes on a hot plate at 110°C to complete the process.

The photoelectric characteristics of the shingled modules fabricated with ECA and Galinstan were confirmed by using light current voltage (I-V) measurements. Those measurements were performed to check the photoelectric characteristics of the shingled modules fabricated with ECA and Galinstan after a thermal cycle (TC) test of 200 cycles to test the durability of both modules [16]. To confirm the effects of the interconnection material and modularization method on the unit cell be measured, the quantum efficiency before and after the TC test and the photoluminescence of both modules.

The difference between the shingled module and the conventional module structures is that in the case of conventional modules, the ribbon and the busbar are connected by soldering when the solar cell is electrically connected, but in the shingled module, they are directly connected by using ECA. Therefore, the contact resistance between the busbar and ECA should be lower than the contact resistance between the busbar and the ribbon [17]. Thus, the characteristics of the shingled module can be compared with those of the conventional module. First, a sample was fabricated to confirm the contact resistance between the busbar and the ECA, and a transmission line measurement (TLM) was used to measure the contact resistance [18]. Ag paste and AgAl paste, which are used as the front and the rear busbars of solar cells, were printed on the entire surface of the silicon substrate, and the ECA was dispensed in lines with a spacing of 10 mm. Figure 3 shows the TLM results for the ECA and the Ag paste and for the ECA and the AgAl paste. The contact resistance between the ECA and Ag was 0.09 $\mu\Omega\cdot cm^2$; the contact resistance between the ECA and AgAl was 6.0 $\mu\Omega\cdot cm^2$, compared to the known contact resistance of the busbar and ribbon used in the conventional module process 120 $\mu\Omega\cdot cm^2$. The contact resistance was confirmed to be very low [19]. However, because the Galinstan paste, which is another interconnection substance, is a liquid metal, the contact resistance could not be measured because the probe and the contact were not set up correctly for the measurement. Because the modules fabricated with ECA and Galinstan showed similar series resistances compared with photocurrent-voltage characteristics in Table 1, the contact resistances between the Galinstan and Ag and between the Galinstan and AgAl did not matter for the fabrication of the module.

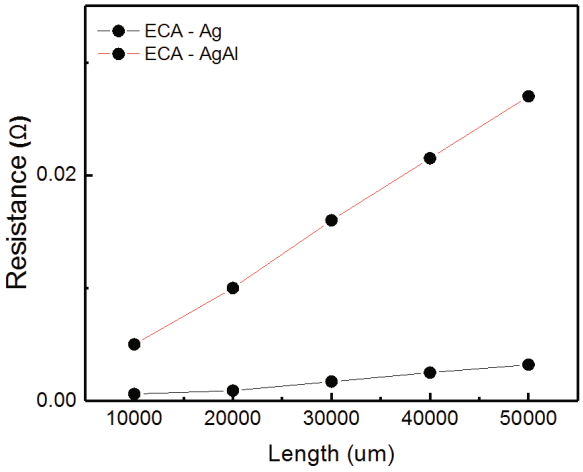

Fig. 3. (Color online) TLM results for the ECA and Ag paste and for the ECA and AgAl paste.

Figure 4 shows the photocurrent-voltage results for the modules fabricated with ECA and Galinstan paste, and Table 1 summarizes the photocurrent-voltage characteristics of both modules. The efficiencies of the modules fabricated using ECA and Galinstan were 18.2% and 18.6%, respectively, and the series resistances were 0.298 Ω and 0.278 Ω, respectively. Because the series resistances of the modules fabricated with ECA and Galinstan were similar, the contact resistance should almost be the same when the interconnection is made with Galinstan.

Additionally, a TC test was performed to evaluate the durability of the interconnection materials in the modules. The TC test was performed by elevating the temperature at a rate of less than 100°C per hour from

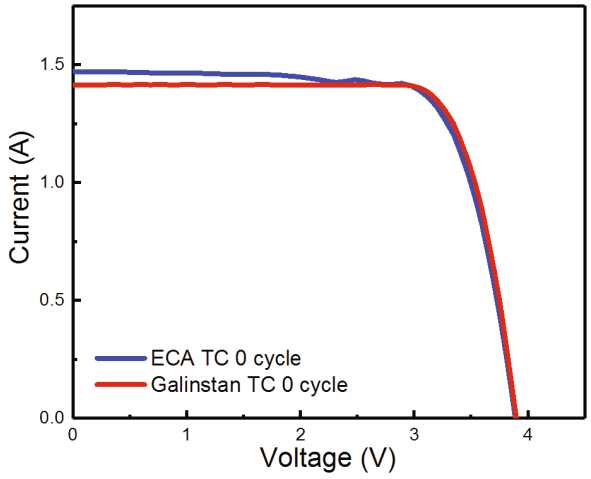

Fig. 4. (Color online) Photocurrent-voltage characteristics of modules fabricated with ECA and Galinstan TC (thermal cycling) after 0 cycle.

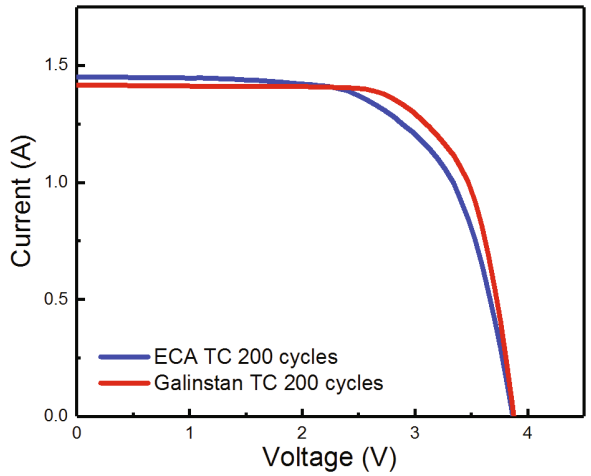

Fig. 5. (Color online) Photocurrent-voltage characteristics of modules fabricated with ECA and Galinstan after TC 200 cycles.

−40°C to 85°C, maintaining the temperature for 10 minutes, lowering the temperature at a rate of less than 100°C per hour from 85°C to −40°C and maintaining the temperature of the module for 10 minutes to check the characteristics of the module. Figures 4 and 5 show the photocurrent-voltage characteristics immediately after the fabrication of modules using Galinstan and the ECA, respectively, after 200 TCs. The efficiency of the module manufactured with Galinstan was 18.6%, which was higher than the efficiency of 18.2% for the module manufactured with ECA, and the series resistances were measured as 0.278 Ω and 0.298 Ω, respectively. In this case, because the resistance components of both modules consisted of the resistance of the cell, the resistance of the interconnection material, and the contact resistance between the cell and the interconnection material, the resistance difference between the two modules was

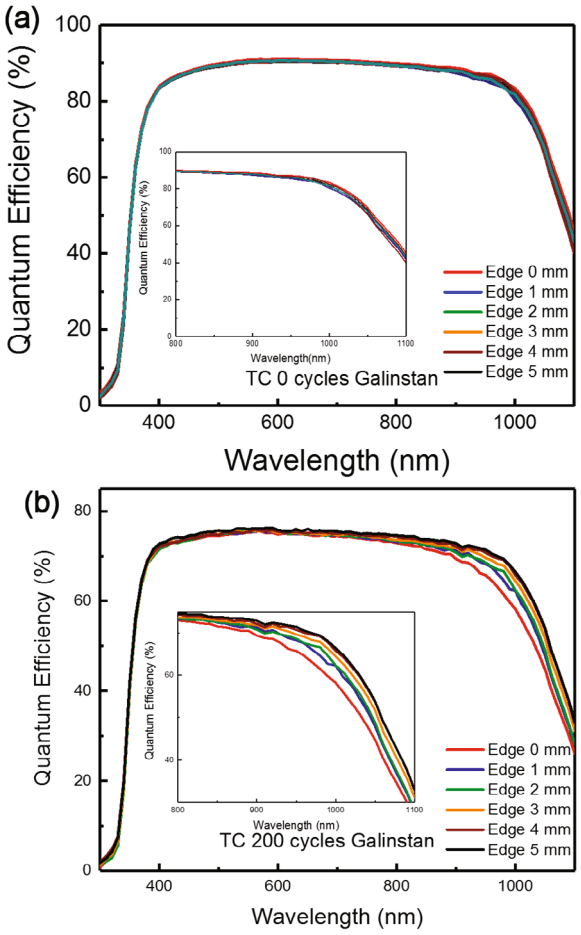

Fig. 6. (Color online) Quantum efficiency before and after thermal cycling using Galinstan. (a) Galinstan paste interconnection module (TC 0 cycles); (b) Galinstan paste interconnection module (TC 200 cycles).

attributable to the interconnection material. Therefore, the contact resistance between Galinstan and the busbar is expected to be lower than the contact resistance between the Ag busbar and ECA, and this finding means that the interconnection resistance is sufficiently low [20].

Both modules showed a decrease in efficiency in the case of 200 TCs. Although the open-circuit voltage and the short-circuit current did not decrease significantly in either of the two types of modules, the efficiencies of the modules decreased due to a reduction in the fill factor. The series resistances of the modules manufactured with ECA and Galinstan after TC tests were 0.387 Ω and 0.270 Ω, respectively. To confirm the cause for the decrease in the short-circuit current, we measured the photoluminescence before and after the thermal cycling. Figures 8 and 9 show the photoluminescence images of the modules fabricated by using ECA and Galinstan, respectively, after 200 TCs. In the module fabricated by using ECA, cracks that had formed in the interconnection area of the cell were evident in the photoluminescence immediately after the fabrication, and several cracks propa-

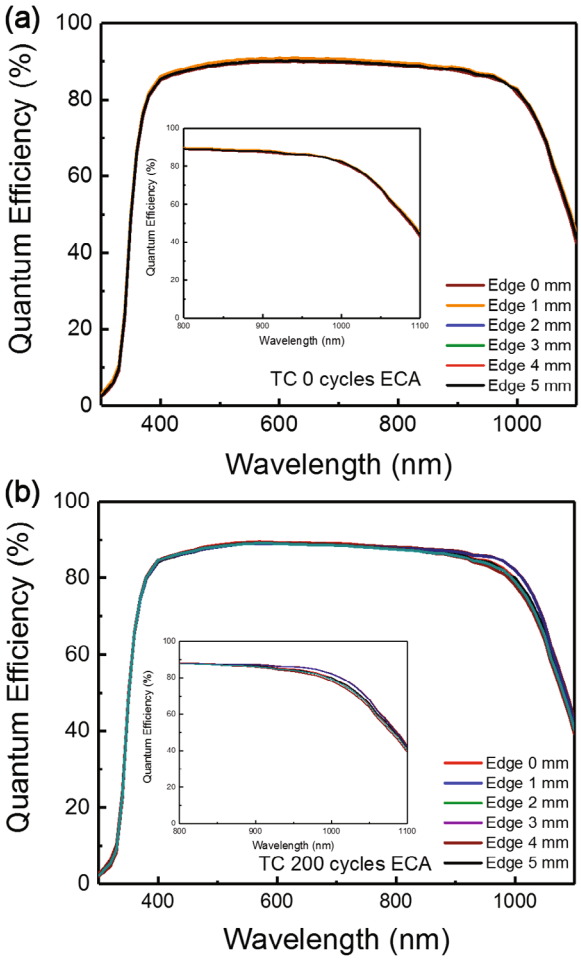

Fig. 7. (Color online) Quantum efficiency before and after thermal cycling using ECA. (a) ECA interconnection module (TC 0 cycles); (b) ECA interconnection module (TC 200 cycles).

gated after the TC test; in addition, the damaged area of the entire cell was also observed. This damage resulted from the following processes: The cracks were generated along the step of the cell by the pressure during the lamination process, the generated cracks propagated during thermal cycling to form a crack from cell to cell, and the series resistance increased as the collected carriers became difficult to collect [21]. In contrast, the module fabricated by using Galinstan did not crack before or after thermal cycling, which result is consistent with almost no change in the series resistance.

For the module manufactured by using Galinstan, the parallel resistance increased while the fill factor decreased. To confirm the cause of the decrease fill factor, the quantum efficiency was scanned from the edge of the cell to the inside in 1 mm intervals. Figures 6 and 7 show the quantum efficiency results before and after the thermal cycling of the modules fabricated using Galinstan and ECA, respectively. Almost no differences were seen in the quantum efficiency based on the

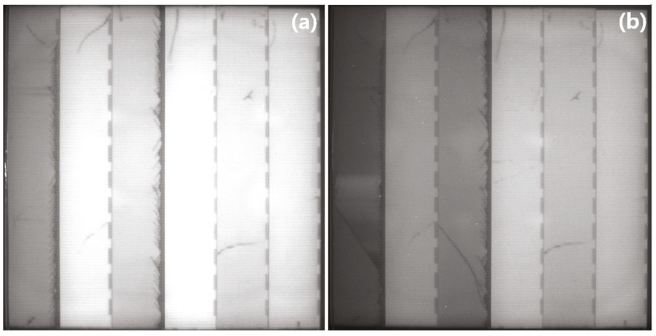

Fig. 8. (Color online) Photoluminescence images (ECA and EVA lamination module). (a) TC 0 cycles and (b) TC 200 cycles.

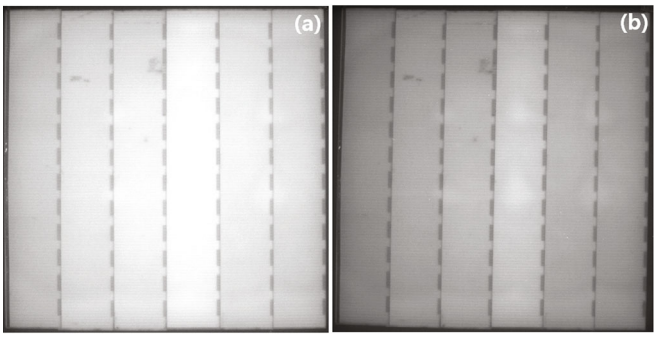

Fig. 9. (Color online) Photoluminescence images (Galinstan and liquid silicone module). (a) TC 0 cycles and (b) TC 200 cycles.

measurement position immediately after the fabrication of the modules using ECA and Galinstan; however, the quantum efficiency decreased in the long-wavelength region because that region was closer to the outside of the cell, even though almost no change occurred in the short-wavelength region. The quantum efficiency is such that the short-wavelength region corresponds to the light-receiving part of the cell, and the long-wavelength region is represented by the area of the whole cell; therefore, the TC test was confirmed not to have affected the light-receiving part of the cell, although this test can affect the lower structure of the cell. Galinstan reacted with the Al paste and corroded the electrode because the quantum efficiency in the long-wavelength region decreased when approaching the area where Galinstan had been applied [22].

III. CONCLUSION

In this research, we fabricated shingled modules for solar cells by using ECA and Galinstan paste as the interconnection materials. The contact resistances between the ECA and the Ag busbar and between the ECA and the AgAl busbar were measured using the TLM method, and the contact resistance between the ribbon and the

busbar was confirmed to be lower than that for the conventional module manufacturing method. Additionally, the initial efficiencies of the modules fabricated using ECA and Galinstan were 18.2% and 18.6%, respectively, and after 200 TCs, efficiencies of 15.7% and 16.8% were obtained, respectively. To investigate the cause of the decrease in efficiency, measured the photoluminescence and were able to confirm that a microcrack occurred in the module made with ECA; this crack propagated after 200 cycles of thermal cycling and diffused inside the cell [22]. However, in the module made using Galinstan, no cracks were found before or after the thermal cycling, and we confirmed that the rear surface recombination increased after the thermal cycling. Therefore, shingled modules can be fabricated by applying new interconnection materials that are different from conventional materials.

ACKNOWLEDGMENTS

The authors would like to thank Mr. Kim for helpful discussions and gratefully acknowledge support by MOCIE through the National R&D Project for Nano Science and Technology. This work was conducted under the framework of Research and Development of the Korea Institute of Energy Research (B8-2421), the New and Renewable Energy Technology Development Program of the Korea Institute of Energy Technology Evaluation and Planning (KETEP) through a grant funded by the Ministry of Knowledge Economy, Korea (Project No. 20163020010890), and the Technology Development Program to Solve Climate Changes of the National Research Foundation (NRF) funded by the Ministry of Science, ICT & Future Planning (2017M1A2A2086911).

REFERENCES

[1] T. Saga, NPG Asia Mater. **2**, 96 (2010).
[2] A. W. Czanderna and F. J. Pern, Sol. Energy Mater. Sol. Cells. **43**, 101 (1996).
[3] M. Mittag, in *44th IEEE Photovoltaic Specialist Conference* (Washington D.C., USA, June 25–30, 2017).
[4] T. H. Jung, H. E. Song, H. K. Ahn and G. H. Kang, Sol. Energy. **103**, 253 (2014).
[5] L. J. Caballero, in *IEEE 4th World Conference on Photovoltaic Energy Conference* (Waikoloa, USA, May 7–12, 2006).
[6] J. Zhao *et al.*, IEEE Electr. Device Lett. **18**, 48 (1997).
[7] D. Tonini, in *35th European PV Solar Energy Conference and Exhibition* (Brussels, Belgium, September 24–28, 2018).
[8] C. P. Wong, in *The First IEEE International Symposium on Polymeric Electronics Packaging* (Norrkoping, Sweden, October 26–30, 1997).
[9] H. J. Lewis and F. M. Coughlan, J. Adhes. Sci. Technol. **22**, 801 (2018).
[10] E. Sancaktar and L. Bai, Polymers **3**, 427 (2011).
[11] D. Y. Shin *et al.*, Sol. Energy Mater. Sol Cells. **180**, 10 (2018).
[12] S. Riegel *et al.*, Energy Procedia **21**, 14 (2012).
[13] P. Baliozian *et al.*, Solar RRL. **2**, 1 (2018).
[14] L. Theunissen *et al.*, AIP Conf. Proc. **1999**, 1 (2018).
[15] G. Beaucarne, in *6th Workshop on Metallization and Interconnection for Crystalline Silicon Solar Cells* (Konstanz, Germany, May 2–3, 2016).
[16] T. Liu, P. Sen and C. Jin, J. Microelectromech Syst. **22**, 1248 (2011).
[17] Y. J. Jeon, D. S. Kim and Y. E. Shin, Int. J. Precis. Eng. Manuf. **15**, 355 (2014).
[18] L. Shen, Z. Y. Tan and Z. Chen, J. Mater. Sci. Eng. A **561**, 232 (2013).
[19] P. N. Vonod, J. Mater. Sci. **22**, 1248 (2011).
[20] S. K. Schröder, in *SiliconPV: 2nd International Conference on Silicon Photovoltaics* (Leuven, Belgium, April 3–5, 2012).
[21] T. Geipel, in *26th European Photovoltaic Solar Energy Conference and Exhibition* (Hamburg, Germany, September 5–9, 2011).
[22] M. Dhimish, V. Holmes, B. Mehrdadi and M. Dales, Adv. Mater. Devices **2**, 199 (2017).
[23] P. Ahlberg *et al.*, IEEE Trans. Electr. Devices **61**, 2996 (2014).